Conf. 9110146 --11

BNL--45043

Laser-Synchrotron Hybrid Experiments
"A Photon to Tickle - A Photon to Poke"

DE92 007611

D.L. Ederer, J.E. Rubensson, D.R. Mueller
National Institute of Standards and Technology
Gaithersburg, MD 20899

R. Shuker
Ben Gurion University
Beer Shiva, Israel

W.L. O'Brien, J. Jai, Q.Y. Dong, T.A. Callcott
University of Tennessee
Knoxville, TN 37996

G.L. Carr
Grumman Corporation Research Center
Bethpage, NY 11714

G.P. Williams, C.J. Hirschmugl
National Synchrotron Light Source
Upton, NY 11973

S. Etemad, A. Inam
Belcor
Redbank, NJ 07701

D.B. Tanner
University of Florida
Gainesville, FL 32611

Abstract

In this paper we present the preliminary results from a new experimental technique to synchronize the pulses from a mode-locked NdYAG laser to the light pulses in the VUV storage ring at the National Synchrotron Light Source (NSLS). We describe a method to electronically change the delay time between the laser pulses and the synchrotron pulses. We also illustrate a method to overlap the synchrotron pulses with the laser pulses in space and time. Preliminary results will be presented for two experiments.

Introduction

While pulsed VUV sources were used in conjunction with lasers in the mid-seventies to study [1] the photo-ionization of excited atoms, multi-color photon experiments, utilizing lasers and synchrotrons, had their beginnings in the late seventies [2]. One possible use of synchrotron-laser hybrid experiments is to probe excited states, and thereby study correlations in multi-electron atoms of electronic states that have the opposite parity of the ground state. In this case a c.w. laser produces an equilibrium population of excited atoms. An example [3,4] of this type of experiment used a c.w. laser produce the excited atoms and the VUV from the storage ring at LURE to study the photoionization of excited atoms. In another experiment a c.w. laser was used at Hasylab to align atoms [5]. The VUV synchrotron light photoionized the atoms, and photoelectron spectroscopy was used to analyze the ionization products. More recently a c.w. laser was used [6] to photodissociate iodine molecules and the VUV beam from LURE was used to photoionize core electrons of iodine. At the Aladdin synchrotron a c.w. laser was also used to induce fluorescence in F centers [7] produced by synchrotron radiation.

For another group of experiments, the time structure of the laser and the synchrotron source are used directly to study dynamical processes. In experiments of this type the pulsed laser would be used in conjunction with the pulsed synchrotron for studies of energy transfer mechanisms in gases and condensed matter. These experiments were first done [2] at the Hasylab when UV from the synchrotron was used to produce an exciton through a valence band excitation, and a pulsed laser was synchronized with the pulses in the synchrotron at 10 Hz. to measure the lifetime of the exciton. Similarly, a pulsed laser was synchronized with the x-rays from the Cornell synchrotron light source to study [8] the pulsed annealing of silicon and a pulsed copper vapor laser running at a few kHz. was

2

synchronized with the NSLS x-ray ring running in the single pulse mode to study [9] band bending in semi-conductors.

All these experiments utilized either a c.w. laser or a laser pulsed at rates slow compared to that of the synchrotron. The first use [10] of a mode-locked laser synchronized with synchrotron pulses was carried out at the UVSOR. In this paper we shall describe our experiments at the NSLS with a mode-iocked laser synchronized to the storage ring light pulses. We would like to present a preliminary report on two experiments. The first is to use VUV photons to populate a core exciton level in an insulator, and photoionize it by the laser. The second is to use the laser to inject carriers in a superconducting material and then use infra red photons from NSLS VUV ring to observe a change in absorption.

Table I identifies some of the dynamical phenomena that can be studied with pulsed light sources. Third generation synchrotron sources will have light pulse widths on the order of a few picoseconds, and present day lasers can produce sub picosecond pulses. At the present time most storage rings are limited to pulse widths of a few hundred picoseconds. Third generation sources will produce a whole new time regime for investigation. They will be especially valuable for dynamical processes such as, molecular vibration and rotation and processes involving the transfer of an electron from one molecular site to another, which have a time duration of order of a picosecond. Present day synchrotrons can be used to study the decay of the excited states in atoms or molecular tumbling in solutions that have time durations of about 10^{-9} seconds [11]. Time durations of 10^{-6} seconds is about the upper practical limit using synchrotrons, because the time for an electron bunch to travel around the ring is of a similar order of magnitude. This

3

is time regime for the decay of metastable excited states and phenomena that involve phosphorescence.

Experimental Apparatus

This technique has been developed to match the high peak flux from synchrotron sources with the high peak power available in mode-locked lasers and use the added dimension of time to study the dynamics of physical processes within the constraints provided by the current generation of synchrotron radiation sources. Furthermore, the duty cycle is increased and the maximum intensity is used effectively for the excitation of processes that have a lifetime of order of nanoseconds for the present day sources. Lasers are powerful but not as broadly tunable as synchrotron radiation (s.r.). In the examples we will show, synchrotron photons as low in energy as 0.1 eV and as high in energy as 70 eV will be used. By developing this technique, we will have the technology in place to exploit third generation synchrotron radiation sources and the faster pulses of greater intensity that will be available from them. An advantage this method has for studying fast events is the detector can be slow. All the timing information is carried by the high speed inherent in the laser and synchrotron.

We have synchronized a mode-locked laser to the string of pulses in the ring by using the r.f. driving the synchrotron source to drive the acoustic modulator in the laser cavity. The laser pulses occur at twice the r.f. frequency. The two trains of pulses, one from the laser and the other from the electrons in the storage ring are locked together with some arbitrary time interval between them. The time interval between the s.r. pulse and the laser pulse can be changed by using an optical delay line or by electrically changing the phase between the r.f. driving the synchrotron and the phase of the r.f. driving the acoustic modulator. The r.f. phase can be

4

changed by applying a voltage to an electrically driven phase shifter. Voltage control of the phase is especially important for dithering the time interval at a low frequency ω, and using phase sensitive detection methods to detect low level signals with greatly enhanced sensitivity. The generic setup is shown schematically in Fig. 1, where a pulse train from a diode and one from the s.r. source overlap at the sample. The sample produces particles, which are detected in some sort of spectrometer, as a result of being excited by one or both of the sources.

The pulses trains from the two sources must overlap in space and time at the sample. The crucial issue of whether these pulses coincide in time and position must be addressed. To solve this problem we put a small photodiode in the sample chamber just behind the sample, as shown schematically in Fig 2. To prevent damage to the diode from the 10 Watts of focussed white s.r. light that is available, we placed a quartz window on the sample holder between the diode and the incoming radiation. The diode was illuminated with white light from the storage ring, whose pulses are 19 ns apart. They have pulse width on the order of 400 ps, which is also the approximate rise time of the photodiode. The pulses from the s.r. source are shown in Fig. 3a and identified in the oscilloscope trace of the diode output by the arrow and the letter, S. There are nine "buckets" of electrons in the ring at NSLS, but only six or seven of them are filled, so there will be six or seven pulses of photons followed by a quiescent period of 60-80 ns until the next string of photon pulses. The laser illuminated the same photodiode. The laser pulses are approximately 9.5 ns apart, and occur at twice the frequency of the synchrotron photons. The laser pulses are identified on the oscilloscope trace by the arrow with the letter L . The doubling of laser pulses is due to ringing in the cable and amplifier. By adjusting the voltage on the electronic phase shifter, we can then bring the laser pulses into time coincidence with the s.r. as shown in Fig. 3b. The s.r.

pulse remains fixed in time relative to the r.f., shown as the sine wave trace of 52.88 Mhz. in Fig. 3a, and 3b, while the laser pulses move in time. The phase change can be calibrated so that the voltage change can be converted to a time change with an accuracy of about 100 ps. By using a small silicon photodiode positioned in situ, the uncertainty in timing at the sample has been reduced to about 100 ps, corresponding to a phase change of a few degrees, and the uncertainty of superimposing the laser pulses and the s.r. pulses has been reduced to a few tenths of a millimeter. Pulses passing through the quartz window change the timing by few ps.

Experimental results

The laser power used at NSLS is about one-half watt at 530 nm which corresponds to 1.4×10^4 watts/cm^2 peak power, yielding a fluence, Q, about 3×10^{20} photons/ cm^2-s at the sample. The fractional change in synchrotron light intensity $\Delta I/I$ produced by the presence of the laser is to a good approximation given by

$$\Delta I/I = Q \sigma \tau$$

Where the quantity τ is the lifetime of the excited state, expressed in seconds, and σ is the cross section, expressed in cm^2 to deplete the excited state by interaction with the laser field. The quantities $\Delta I/I$, Q, and σ can be measured or calculated thus yielding the lifetime τ. We can estimate the range of τ that is available to this measurement technique by substituting the known value of Q and making an educated guess for the cross section σ. We assume a cross section of about 10^{-17} cm^2 and multiply it by the laser fluence, Q. The product of the two numbers is 3×10^5. To measure times of order picoseconds the quantity $\Delta I/I$ must be measured to one part in 10^{-6}. Measuring a change in intensity as small as a part in a million is a difficult task and usually requires some sort of phase sensitive detection scheme. Of course this constraint is relaxed if the lifetime is longer or the cross section is larger.

We tried this technique out on a couple different systems. The rest of the paper will be devoted to a description of our results. For the first measurement, we chose the exciton in aluminum oxide. In Fig.4 we see the absorption spectrum of aluminum oxide [12] obtained with a high sensitivity spectrometer [13] mounted on the VUV ring at the NSLS. The abscissa is given as an energy relative to the valence band maximum, VBM. A very prominent prominent two peak structure, labeled S , corresponds to a transition from a 2p core state to an excited s state which lies in the band gap of aluminum oxide. This core exciton has an excitation energy of 79 eV and corresponds closely to the 3s level in Al^{3+}. We wish to measure the interaction of the exciton with the laser field by measuring a change in the reflectivity of the sample. Other features in the spectrum correspond to structure in the conduction band related to core excitations in the aluminum ion. In Fig. 5 the energy scale has been expanded around the exciton. The $^2P_{3/2}$, and $^2P_{1/2}$ excitons are labeled G and H respectively. The neighboring band gap, and conduction bands have been labeled N, I, J respectively.

Reflectivity measurements were made as a function of time between the laser excitation pulse and the synchrotron light pulse. Typical integration time for one spectrum was about ten minutes. The spectra were processed and the counts in the energy bands G through N were added up. In Fig. 6, we show the counts in the energy bands corresponding to the exciton, (G and H), and the integrated counts in the conduction bands (I and J), divided by the integrated count in the band gap (N), which are assumed to be unaffected by the laser. Each unit on the abscissa corresponds to a time delay change of 150 ps between the laser pulse and the photon pulse from the synchrotron source. For a time scale of approximately 600 ps, occurring between 6 and 10 units, the laser overlaps the synchrotron pulse as measured in a separate experiment. In Fig. 7, the ratios are plotted on an expanded scale for the $^2P_{3/2}$ exciton (Fig 7a), and for band structure lying just above the

conduction band minimum (Fig. 7b). Other than a long term drift, no change greater than 0.3% is seen in the quantity $\Delta I/I$. This places an upper limit of about 10^{-8} s on the lifetime of the excited states. It is believed that these excitons have lifetimes several orders of magnitude shorter than this. To push the measurements to shorter times phase sensitive detection schemes will have to be used, which will produce a gain in sensitivity of several orders of magnitude. To obtain more photons, it is possible to Q switch the laser and gain somewhat in signal to noise, at the expense of a considerably longer integration time, because of the reduced duty cycle.

The next experiment that was used to test this pump-probe technique involved transporting the doubled mode-locked synchronized pulses via an optical fiber to the infrared beam line, U4-IR, at the NSLS [14]. One system we have chosen for study is the high-Tc superconductor $YBa_2Cu_3O_{7-\delta}$ (YBCO). The far infrared transmission through a superconducting film decreases toward longer wavelengths due to screening by the superfluid carriers (pairs). Photons of visible light break the pairs, reducing their density and increasing the long wavelengths transmission. Fig. 8 shows the normalized, photo-induced change in transmission ($\Delta T/T$) for an epitaxical YBCO film on $LaAlO_3$ at 80 K. In all cases the laser pulses cause the transmission to increase, especially at the longer wavelengths. The broken curves illustrates the effect of varying the pump-to-probe delay times. The small variation with delay time is due to the recombination of excitations into pairs, which takes place in a few nanoseconds, and is probably governed by the characteristic time for phonons to escape from the film into the substrate. The solid curve is the change in transmission for a 3 K temperature rise and its similarity to the photo-induced data demonstrates that much of the signal can be attributed to heating of the substrate.

Acknowledgements

8

References:

[1] T. Lucatorto and T. McIlrath, Phys. Rev. Lettrs. 37 (1976) 428.

[2] V. Saile, Appl. Opts. 19 (1980) 4115.

[3] J.M. Bizau F. Wuilleumier, D.L. Ederer, J.C. Kerrer, J.L. LeGouët, J.L. Picqué, B. Carré, and P.M. Koch, Phys. Rev. Lettrs.55 (1985) 1281.

[4] J.M. Bizau F. Wuilleumier, D.L. Ederer, J.C. Kerrer, J.L. LeGouët, J.L. Picqué, B. Carré, and P.M. Koch, Phys. Rev. Lettrs.57 (1986) 306.

[5] M. Meyer, B. Müller, A. Nunnemann, Th. Prescher, E.v. Raver, M. Richter, M. Schmidt, B. Sonntag, and P. Zimmermann. Phys. Rev. Lettrs. 59 (1987) 2963.

[6] P. Morin et al , Phys. Rev. Lettrs.,*xxx*, isss (1987).

[7] F. Brown,B.R. Sever, and J.P. Stott, Phys. Rev. Lettrs., 57 (1986) 2279.

[8] B.C. Larson, C.W. White, T.S. Noggle, and D. Mills, Phys. Rev. Lettrs.,48 (1980) 337.

[9] J. P. Long H.R. Sadeghi, J.C. Rife, M.N. Kabler , Phys. Rev. Lettrs. 64 (1990) 1158.

[10] T. Mitany, H. Okamoto, Y. Takagi, M. Watanabe, K. Fukui, S. Koshihara, C. Ito, Rev. Sci. Instrum.60 (1989) 1569.

[11] I.H. Munro, I. Pecht, and L. Stryer, Proc. Nat. Acad. Sci. (USA), Biochem. 76 (1979) 56.

[12] W.L. O'Brien, J. Jia, Q.-Y. Dong, T.A. Callcott, J.-E. Rubensson, D.L. Mueller, and D.L. Ederer, Phys. Rev. 44 (1991) 1013.

[13] T.A. Callcott, K.L. Tsang, C.H. Zhang, D.L. Ederer, and E.T. Arakawa, Rev. Sci. Instrum. 57 (1986) 2680.

[14] Gwyn P. Williams, Int. J. Infrared Millimeter Waves, 5 (1984) 829.

Figure Captions

Fig. 1: Schematic representation of the apparatus to synchronize a Nd:YAG mode-locked laser to the light pulses from a storage ring. SHG is the second harmonic generation module. The r.f. phase is shifted electrically to adjust the time interval between the synchrotron light pulses and those from the laser.

Fig. 2: Schematic diagram of the detector system to superimpose the synchrotron pulses in space and time. The diode has an area of $1mm^2$ and is located behind a quartz plate to reduce the radiation power load on the diode. The presence of a signal indicates spatial superposition at the sample as the diode is located in the vacuum chamber on the sample plane. Viewing the signal on an oscilloscope allows the time interval Δt between the synchrotron pulse and the laser pulse to be measured.

Fig. 3: a) Upper trace: laser and synchrotron pulses falling on a small diode. The synchrotron pulses, occurring every 18.9 ns are labeled S. The laser pulses occurring at half the time interval are labeled L. Lower trace is the synchrotron r.f. having a frequency of 52.88 MHz.
b) The laser and synchrotron pulses are in time coincidence. Note the synchrotron pulse remains fixed in phase relative to the r.f. while the laser pulses shift into coincidence as the r.f. phase was adjusted.

Fig. 4: The absorption spectrum of Al_2O_3 near the aluminum $L_{2,3}$ edge obtained from Ref. 12. The feature, labeled S, is the 2p core exciton occurring at a photon energy of about 79 eV.

Fig. 5: The energy scale has been expanded around the exciton. The $^2P_{3/2}$, and $^2P_{1/2}$ excitons are labeled G and H respectively. The neighboring band gap, and conduction bands have been labeled N, I, J respectively.

Fig. 6: The ratio of counts integrated in region G, H, I, J to region N, the band gap, shown as $\bigcirc$, $\square$, $\triangle$, and $\times$, respectively. The time difference between the synchrotron pulse and the laser pulse is the abscissa. Each unit is 150 ps. Coincidence between the synchrotron pulse occurs between 6 and 8.

Fig. 7: a) The ratio of the integrated count for $^2P_{3/2}$ exciton (G) to the count in the band gap (N) is plotted on an expanded scale.

b) The ratio of the integrated count for band structure lying just above the conduction band minimum (I) to the count in the band gap (N). The time difference between the synchrotron pulse and the laser pulse is the abscissa. Each unit is 150 ps. Coincidence between the synchrotron pulse occurs between 6 and 8.

Fig.8: Fig. 8 shows the normalized, photo-induced change in transmission ($\Delta T/T$) for an epitaxical YBCO film on $LaAlO_3$ at 80 K as a function of the wavenumber. The solid line is the calculated response for laser heating of the film.

Table I:

Time Range

Time (Length)	Phenomenon	Technique
10^{-15} (3000Å)	Photon absorption-Emission	Laser
	Electron emission	
10^{-12} (0.3 mm)	Molecular rotation	Laser
	Molecular vibration	Streak camera
	Electron Transfer	Phase shift
	Exciton migration	Synchrotron
	Collisions in gases and liquids	
10^{-9} (30 cm)	Fluorescence	Laser
	Molecular tumbling in solution	Flash lamps
		Synchrotron

Synchrotron pulses

19 ns

SiO$_2$

Δt

Laser pulses

19 ns

small photodiode in
vacuum chamber

Fig. 2

a)

b)

18.9 ns

Counts

Photon Energy (ev)

150r
4.170
3.150

N G H I J
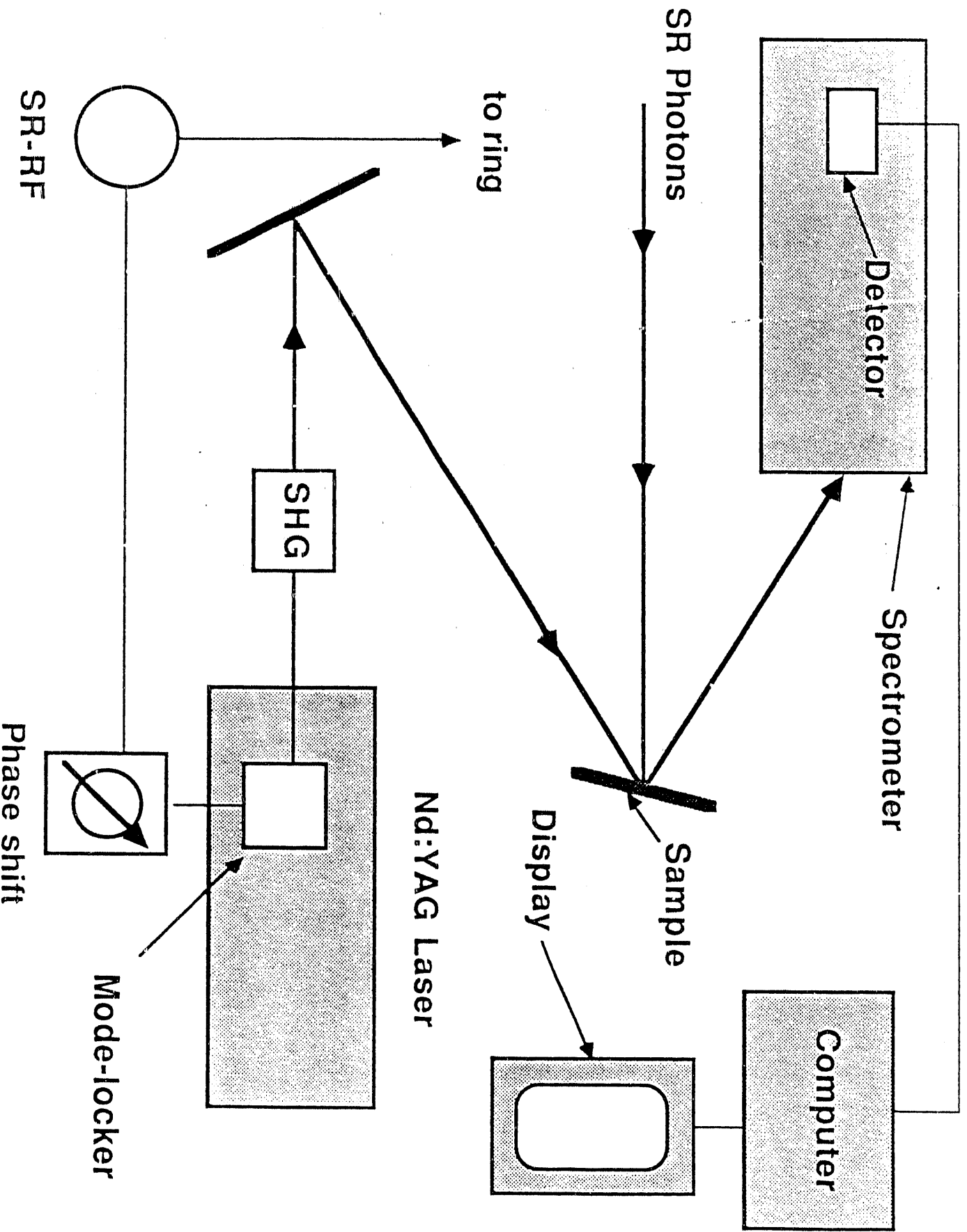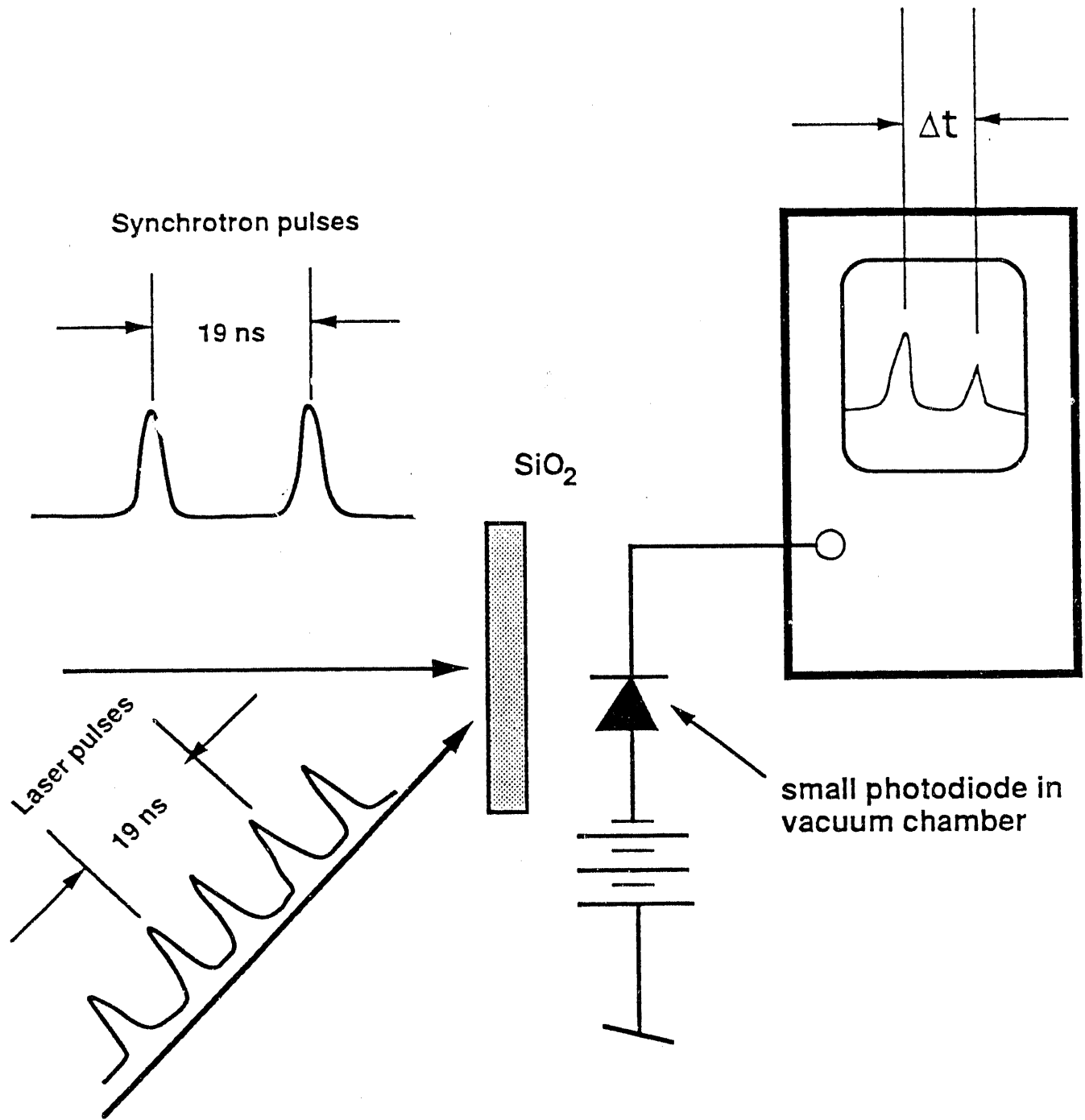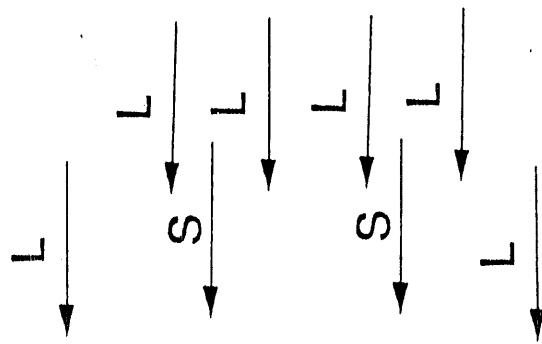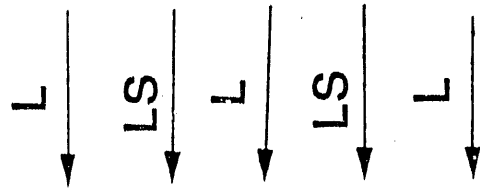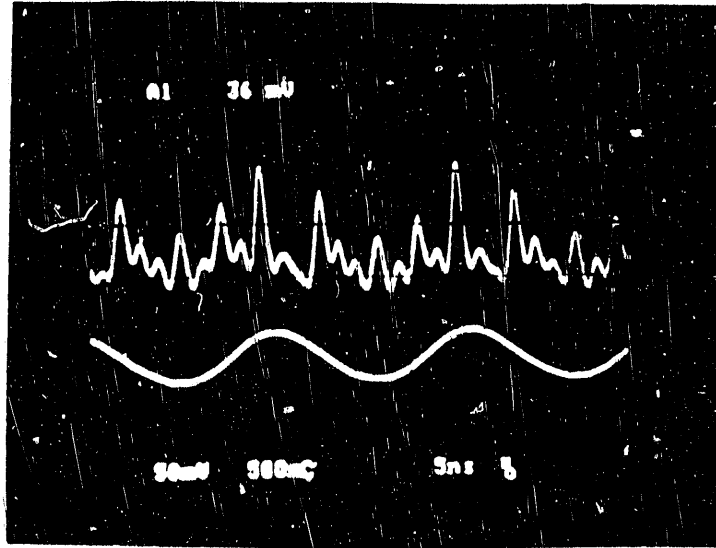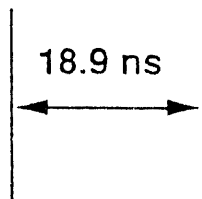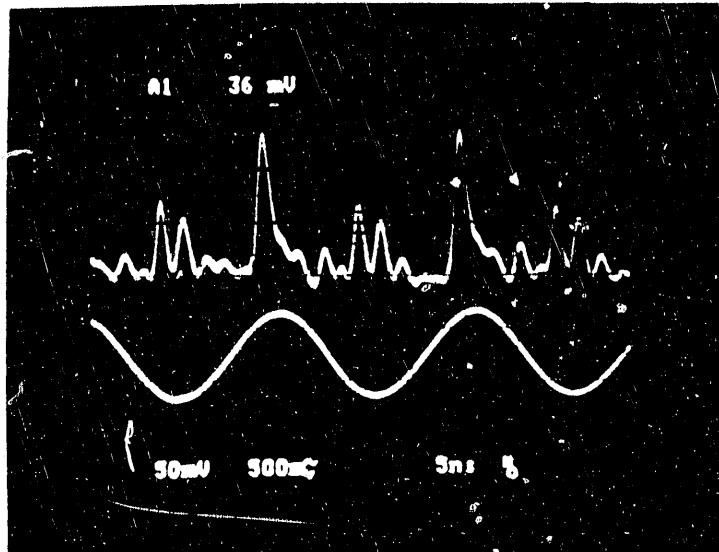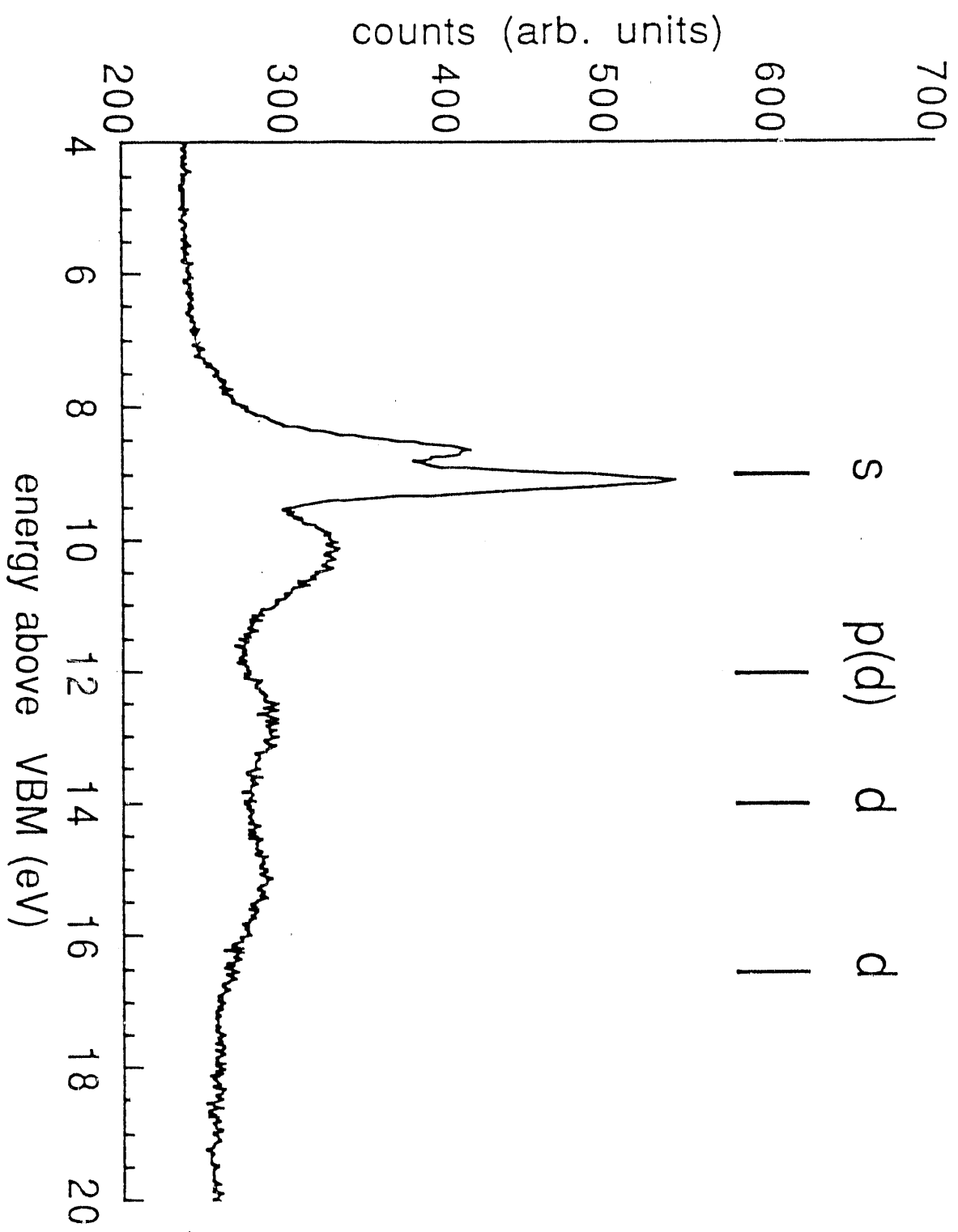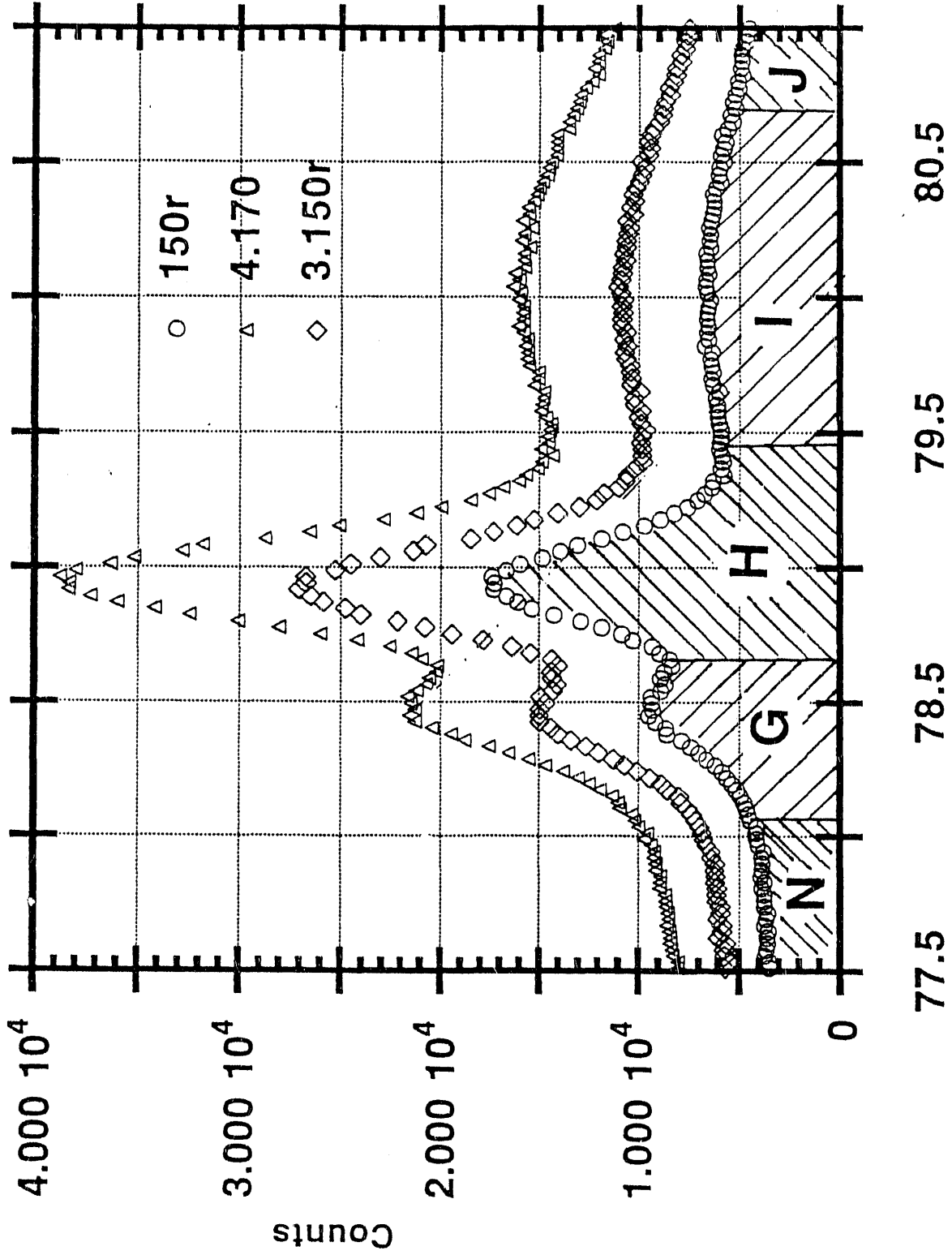
Laser-synchrotron coincidence
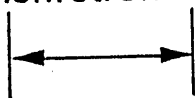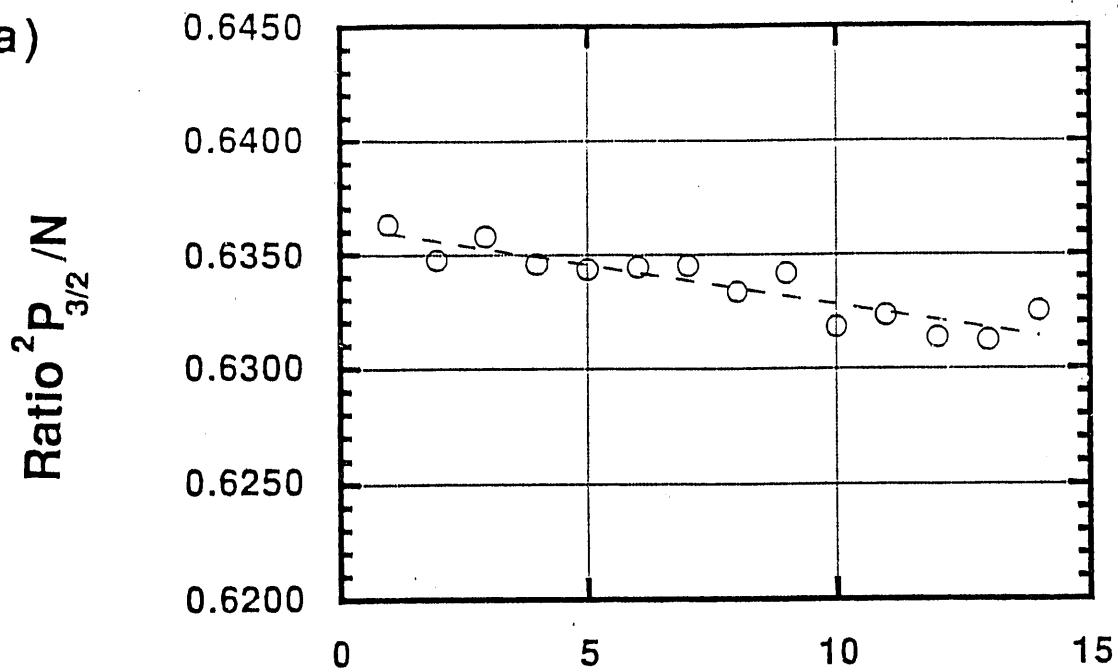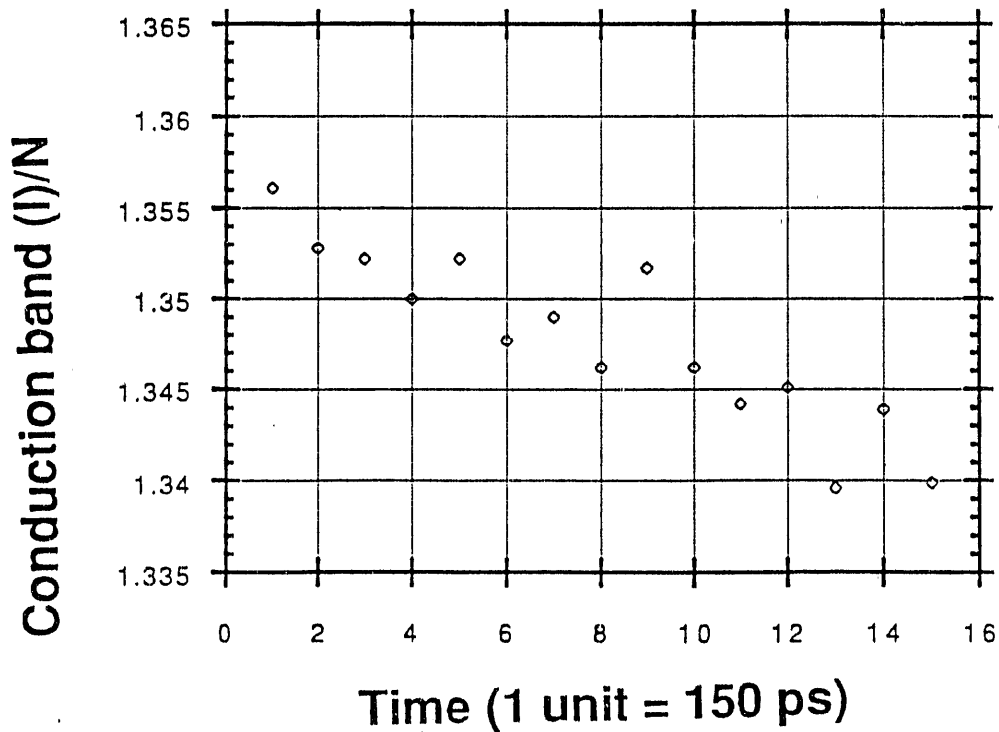
Time-resolved (pump-probe) Far-Infrared Spectroscopy

YBa$_2$Cu$_3$O$_{7-\delta}$ Film on LaAlO$_3$ (T=80K)

- - - - - 1 ns
- - - 4 ns
——— 8 ns
········· 9 ns

——— $\Delta T/T$ for 3K temp. rise

$\Delta T/T$

Frequency [cm^{-1}]

40   60   80   100

0.00   0.05   0.10   0.15

END

DATE
FILMED
3/18/92